

# Expanding Application of Immobilized *Candida Antarctica* Lipase B: A Green Enzyme Catalyst for Knoevenagel Condensation Reaction

Cuie Wang<sup>1\*</sup>, Ning Wang<sup>1</sup>, Xinhua Liu<sup>1</sup>, Peng Wan<sup>1</sup>, Xinwei He<sup>2</sup>, and Yongjia Shang<sup>2\*</sup>

<sup>1</sup>College of Textile and Clothing, Anhui Polytechnic University, Wuhu 241000, China

<sup>2</sup>College of Chemistry and Materials Science, Anhui Normal University, Wuhu 241000, PR China

(Received March 18, 2018; Revised June 11, 2018; Accepted June 14, 2018)

**Abstract:** We propose a green synthesis of benzopyran compound based on immobilized lipase. Firstly, by using a combined electrospun membrane and biocompatible chitosan, we show that the chitosan-functionalized electrospun PMA-co-PAA fibrous membrane can provide effective anchoring sites for immobilization of the *Candida antarctica* lipase B (CALB), and a maximum loading amount of CALB (152 mg/g) can be achieved. Then, the resulting membrane displays enhanced stability in catalyzing Knoevenagel condensation reaction of salicylaldehyde with active methylene compound in mixed aqueous-organic media. The catalytic activity and stability of the CALB on chitosan-modified fiber is better than its non-immobilized counterpart. Furthermore, this immobilized CALB catalyst still retained about 45 % of the initial activity after 5 cycles, which potentially had implications for the design of “green” enzyme catalyst for sustainable organic synthesis.

**Keywords:** *Candida antarctica*, Lipase B, Immobilization, Green catalyst, Knoevenagel condensation

## Introduction

Green chemistry refers to the promotion of environment-friendly, sustainable, and waste-minimizing chemical process [1]. Application of green catalyst is one of the important methods to achieve green chemistry. As an alternative green catalyst, enzyme has been gaining importance in the synthesis of organic compounds due to its superior chemo-, regio-, and stereoselectivity [2-4]. Enzyme has proved to be better biocatalysts for various reactions such as esterification, acylation [5] and hydrolyses triglyceride [6]. Recently, enzyme promiscuity [7], provides new tools for organic synthesis [8-10]. To the best of our knowledge, some promiscuous biocatalytic basic reactions and different types of enzyme promiscuity such as Aldol addition [11], Michael addition [12], racemisation [13] epoxidation [14], condensation reaction [15] and multi-component reaction [16] have been reported. Nevertheless, more useful reaction systems are relatively scarce.

Knoevenagel condensation refers to one of the most important reactions employed for the construction of carbon-carbon double bonds in organic synthesis. It has been applied in the synthesis of important chemical intermediates, pharmaceuticals, polymers, cosmetics, and perfumes. Traditionally, Knoevenagel condensation is carried out in the presence of common bases [17], such as ammonia, primary or secondary and tertiary amines, all of which are difficult to recover. Therefore, various heterogeneous catalysts for Knoevenagel reaction [18,19], such as solid acid-base, copper metal surfaces, and ionic liquids, have been reported. Although these strategies can facilitate catalyst separation, they are still suffering from harsh reaction condition and

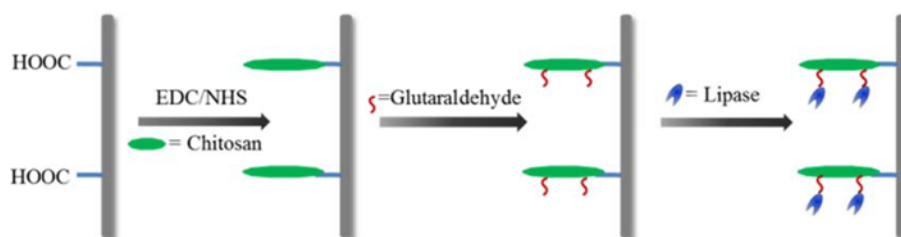
environmental problems. Lipase has been considered as a promising green catalyst in Knoevenagel condensation due to mild reaction condition [20-23].

Nevertheless, the application of lipase often has two major limitations. Firstly, free lipase lacks long-term operational stability and recoverability, and the recovery is also difficult. Secondly, the catalytic activity of lipase in organic system is remarkably lower [24]. These drawbacks can be solved by the use of immobilized lipases [25]. Recently, electrospun fibrous membranes have been applied for enzyme immobilization [26,27], because they are not only highly porous and mechanically flexible but also possess high surface-to-mass ratios. Thus, it allows for faster flux rates than common membranes, which is beneficial to the organic synthesis. However, fibrous membranes are generally nonionic and can be dissolved in organic solvents through non-ionic interactions between solute and solvents, thus limiting their application in organic reaction. Chitosan (CTS) is a kind of polyelectrolyte biopolymers, which possess many ionisable groups. For instances, amine and carboxylic functional groups of CTS can be ionized to carry positive or negative charges that result in CTS insoluble in many organic solutions. Moreover, chitosan (CTS) possesses distinct properties, such as biocompatibility, nontoxicity, and abundant NH<sub>2</sub> groups for anchoring enzymes. Accordingly, the CTS can modify fibrous membrane for binding enzyme with improved enzyme loading and activity, furthermore, CTS makes the fibrous membrane anchored lipase have a promising application in green organic synthesis.

In this work, a CTS-functionalized poly(methyl acrylate-co-acrylic acid) fibrous membrane (CTS@ PMA-co-PAA) was designed to immobilize CALB (Scheme 1). The chitosan can provide the CALB with a biocompatible environment to withstand considerable harsh pH (4-10) and temperature (20-60 °C) conditions. The CALB immobilized on CTS@

\*Corresponding author: cuiewang@126.com

\*Corresponding author: shyj@mail.ahnu.edu.cn



**Scheme 1.** Schematic illustration of the immobilization processes of CALB on electrospun fibers.

PMA-co-PAA can be successfully employed as an environmental-friendly catalyst to synthesize benzopyran compound. When the immobilized CALB was used as a catalyst for the Knoevenagel condensation of salicylaldehyde with active methylene compound, a significantly improvement of the catalytic activity and stability is achieved compared with free CALB. Furthermore, a possible enzyme catalysis mechanism was proposed.

## Experimental

### Materials and Instrumentation

CALB was purchased from Chuangke Biological technology Co. Ltd. (Hangzhou, China). Bovine serum albumin (BSA) protein was purchased from Sigma-Aldrich. Unless otherwise noted, all chemicals and reagents for chemical reactions were obtained from Shanghai aladdin Biological technology Co. Ltd. and used without further purification. Deionized water was used in all experiments. All other chemicals were of analytical grade and were used as received. Deionized water was used in all experiments.

Electrospinning was carried out to prepare PAA-co-PMA fiber with a working distance of 15 cm from the tip of the syringe needle to the grounded collector. The high-voltage supplier (DW-P503-1AC, Tianjin, China) provided an applied voltage of 18 kV. Organic reactions were monitored by thin layer chromatography using an UV-lamp for visualization. The  $^1\text{H}$ NMR spectra were recorded on Varian Mercury 300 spectrometer (300 MHz). Data for  $^1\text{H}$ NMR were reported in the conventional form: chemical shift ( $\delta$  ppm), multiplicity (s=singlet, d=doublet, t=triplet, m=multiplet, br=broad), coupling constant (Hz). Typical scanning electron microscopy (SEM) images were performed by using a Hitachi S-4800 SEM (Tokyo, Japan). Fourier transform infrared (FTIR) spectroscopies were carried out with a Shimadzu IR Prestige-21 FTIR spectrophotometer.

### Preparation of CTS@PMA-co-PAA Fiber

Synthesis of PMA-co-PAA fiber was according to our previous report [19]. Then the membranes were placed in 2 mL EDC/NHS solution (0.1 M EDC and 0.2 M NHS) at 25 °C for 1 h. After reaction, the membranes were rinsed with water. Then the activated membranes were submerged in 3 mL of CTS solution and shaken gently at 25 °C for 4 h.

### Immobilization of CALB onto the CTS@PMA-co-PAA Fiber

10 mg of CTS@PMA-co-PAA fibrous membranes were immersed in 4 mL GA solution (8 wt %) for 3 h at 25 °C under shaking condition. Then the activated membranes were submerged in 3 mL of CALB solution (6 mg/mL) and shaken gently at 25 °C for 2 h. Subsequently, the immobilized-enzyme catalysts of CALB-CTS@PMA-co-PAA were obtained after rinsing with the PBS until no soluble protein was detectable. Finally, CALB-CTS@PMA-co-PAA was stored at 4 °C prior to use. The protein concentrations were determined by Bradford's method [28].

### Enzyme Activity Measurement

The specific activities of free CALB and immobilized CALB were examined by the hydrolysis of olive oil, respectively. In detail, the reaction mixture containing emulsion (2 mL), phosphate buffer (3 mL, 0.025 M, pH 7.5) and free CALB (0.1 mL) or immobilized CALB (80 mg) was incubated for 5 min at 37 °C under continuous agitation. The reaction was stopped by the addition of 10 mL of toluene. The liberated fatty acid released from olive was determined by using UV-752 spectrophotometer. One international unit (IU) of activity was defined as the amount of enzyme required to liberate 1 mmol of free fatty acid per minute under the conditions described above.

### CALB-catalyzed Knoevenagel Condensation Reactions

Ethyl acetoacetate (1 mmol) and salicylaldehyde (1 mmol) were added to 8 mL  $\text{CH}_3\text{OH}/\text{H}_2\text{O}$  solution. The resulting mixture was stirred at 60 °C for 5 h. After that, the immobilized CALB was collected for the next cycle of condensation, the mixture was extracted with  $\text{CH}_2\text{Cl}_2$  (30 mL), and washed with water for three times. The organic layers were collected, dried by anhydrous  $\text{Na}_2\text{SO}_4$ , and evaporated in vacuum. The residue was purified with column chromatography on silica gel (300-400 mesh) ( $\text{EtOAc}/\text{hexane}$ , 1/20, v/v) yielding pure product as white solids.

## Results and Discussion

### Characterization of Materials

The microstructures and size distributions of pristine PMA-co-PAA, chitosan (CTS) modified PMA-co-PAA

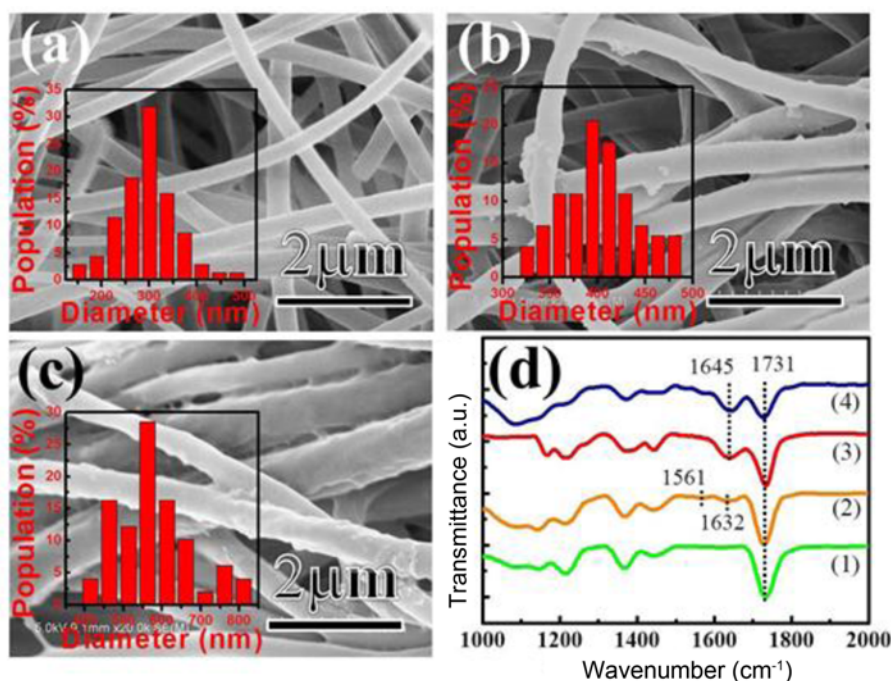


**Figure 1.** SEM images and size distributions of the pristine PMA-co-PAA (a), PMA-co-PAA@CTS (b), PMA-co-PAA@CTS-CALB (c), respectively, and their corresponding FTIR spectra (d).

(denoted as PMA-co-PAA@CTS), and CALB immobilized PMA-co-PAA@CTS (denoted as PMA-co-PAA@CTS-CALB) were monitored by scanning electron microscopy (SEM). According to Figure 1(a)-(c), throughout the immobilization processes, the fibrous morphologies were well maintained, whereas the size distributions of the fibers were increased remarkably. As shown in Figure 1(a), the main size distribution of the pristine PMA-co-PAA fibers is about 300 nm. In case of CTS-modified PMA-co-PAA fibers, the increase of their main size distribution can be observed (PMA-co-PAA@CTS ~400 nm). After immobilization of the CALB, as displayed in Figure 1(c), the PMA-co-PAA@CTS-CALB fiber shows a continuous increase of size distribution (average diameter: ~550 nm). Additionally, the pristine electrospun PMA-co-PAA and PMA-co-PAA@CTS fibers are relatively slender and homogeneous, while the CALB immobilized fibers show a superficial roughness surface. As a result, the main differences lie in the obvious increase of average diameter which may confirm the successful linking of the CALB proteins on the electrospun fibers with high loading amount.

The step-by-step immobilization of chitosan and CALB on the surface of PMA-co-PAA@CTS was confirmed by Fourier Transform Infrared (FTIR). Figure 1(d) exhibits the FTIR spectra of pristine PMA-co-PAA fiber (1), PMA-co-PAA@CTS (2), PMA-co-PAA@CTS-GA (3), and PMA-co-PAA@CTS-CALB (4), respectively. The pristine PMA-co-PAA fiber displays a broad band at 1731 cm<sup>-1</sup> (Figure

1(d(1))), which could be attributed to the stretching vibration of C=O groups in ester and carboxyl. After anchoring of CTS on the PMA-co-PAA (Figure 1(d(2))), typical amine (CONH<sub>2</sub>) group at 1632 cm<sup>-1</sup> and 1561 cm<sup>-1</sup> could be detected, respectively. In the case of GA-activated PMA-co-PAA@CTS (Figure 1(d(3))), the characteristic stretching vibration at 1645 cm<sup>-1</sup> could be assigned to the C=N groups [29]. Besides, the vibrational spectra from C=O groups of PMA and GA overlap with each other at 1731 cm<sup>-1</sup>. After immobilization of CALB (Figure 1(d(4))), the main difference lies in the significant decrease of peak intensity of C=O groups at 1731 cm<sup>-1</sup>. This is possibly because the -CHO group of PMA-co-PAA@CTS-GA reacts with the -NH<sub>2</sub> group of CALB. Furthermore, owing to the formation of C=N bond between the PMA-co-PAA@CTS-GA membrane and the CALB, the characteristic C=N stretching band at 1645 cm<sup>-1</sup> is increased.

#### Activity and Stability of Free and Immobilized CALB

The efficiency of the immobilization was expressed by the amount of CALB bounded on supports of unite mass and the protein concentration was determined by the Bradford method. The catalytic activities of free and PMA-co-PAA@CTS-immobilized CALB were examined by the measurement of the fatty acid that generates from the hydrolysis of olive oil according to a previous report. The maximum activities of the free and PMA-co-PAA@CTS-immobilized CALB under optimal condition were set as 100 %, while the

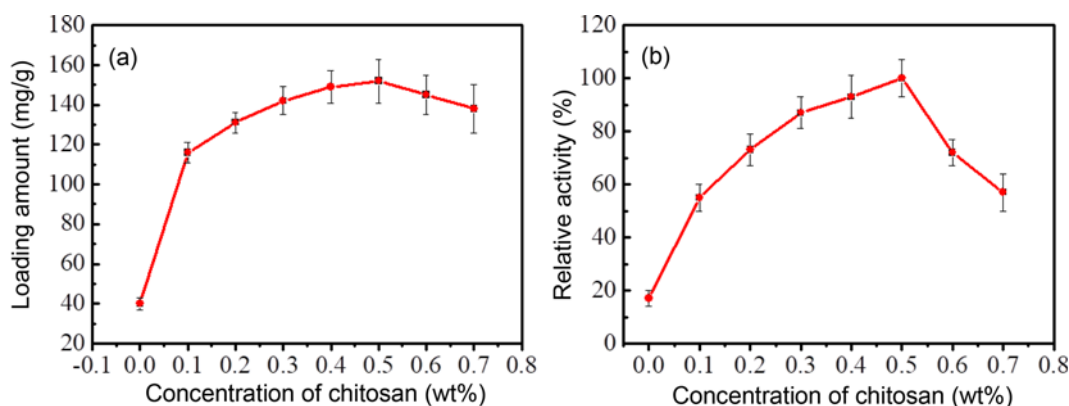


**Figure 2.** The effect of the CTS concentration on the CALB loading amount (a) and activity (b), respectively.

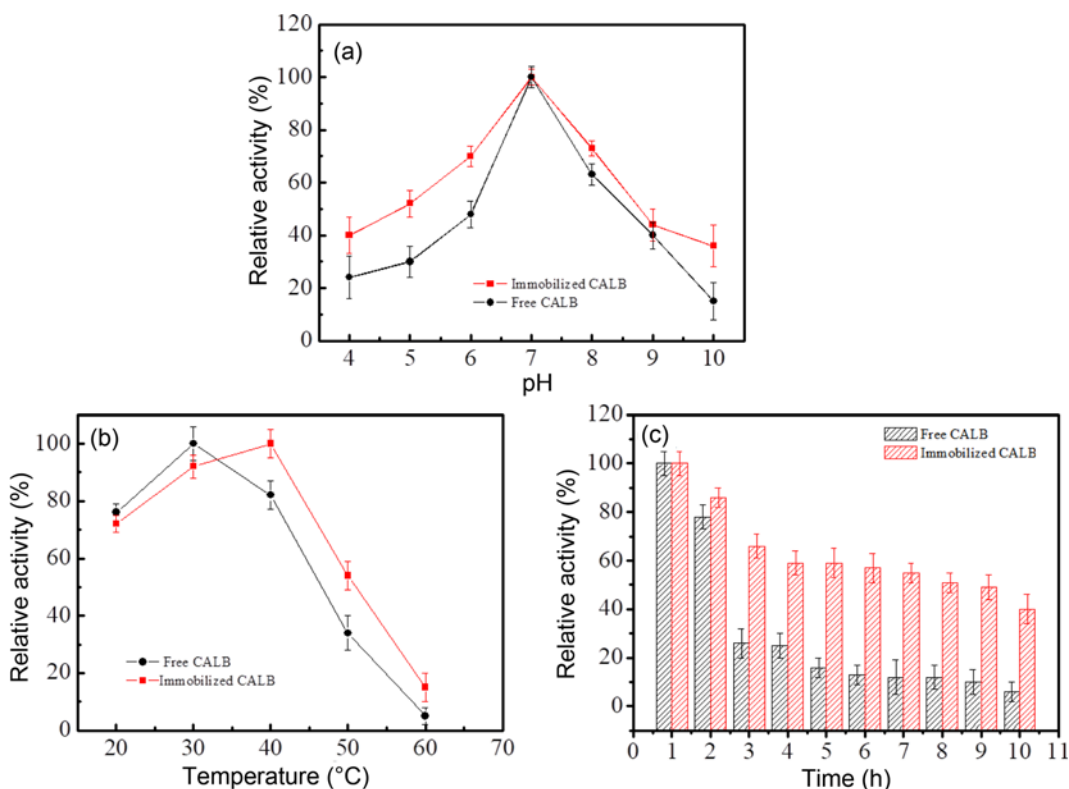


**Figure 3.** Effects of the pH (a), temperature (b), and storage duration at 60 °C, (c) on the activity of the free and immobilized CALB.

activities obtained from other conditions were expressed as relative activities.

Figure 2(a) shows the effects of the CTS concentration on the CALB loading amount. There was a significant threefold increase in mass loading of the CALB can be achieved on the CTS-functionalized electrospun PMA-co-PAA fibrous membrane. This may be due to the fact that the  $-NH_2$  groups of CTS can provide multiple sites for binding CALB. When PMA-co-PAA@CTS was obtained at CTS concentration of 0.5 wt%, a maximum loading amount of CALB (152 mg/g) can be achieved. However, the loading amount of CALB

gradually decreases if the support of PMA-co-PAA@CTS was obtained by increasing the CTS concentration from 0.5 to 0.7 wt%, which is probably due to steric effects of CTS. Figure 2(b) shows the influence of the CTS concentration on the CALB activity. An increase in CTS concentration from 0 to 0.5 % leads to an increased activity of the immobilized CALB from 17 % to 100 %, and then decreases with further increasing CTS concentration. These results could be attributed to the increase of the binding efficiency of the CALB.

Figure 3(a) illustrates the impact of pH values on the olive

oil hydrolytic reaction by using free and immobilized CALB. According to Figure 3(a), although both the immobilized and free CALB reached the optimized activity at a pH of 7, the PMA-co-PAA@CTS-CALB exhibited a higher residual activity than that of free CALB at other pH value. Therefore, the pH stability of CALB can be effectively increased by the immobilization. One possible explanation is that the protective function of the CTS microenvironment results in the improved CALB tolerance to harsh pH conditions.

In usual models of thermal deactivation, an active CALB suffers a reversible or irreversible structure change to generate a catalytically inactive form. The thermal stabilities of the free and immobilized CALB can be presented in Figure 3(b). The immobilized CALB shows better thermal stability than the free CALB which can easily undergo conformation transition and aggregation. However, the thermal stability decreases with the increase in temperature, probably because the disturbance of globular structure of the protein leads to protein unfolding and the loss of activity. According to the finding, PMA-co-PAA@CTS-CALB retains their enzymatic activity by 4 times higher compared to free CALB at 60 °C. Although the heat could reduce conformation flexibility of free and immobilized CALB, the immobilized CALB could still perform a more efficient enzymatic activity than the free CALB.

Considering the practical application, the thermal storage stabilities of free and immobilized CALB were also examined. As shown in Figure 3(c), both free CALB and PMA-co-PAA@CTS-CALB are partly inactivated at 60 °C within 10 hours. Compared with the PMA-co-PAA@CTS-CALB, free CALB's inactivation rate is considerably higher. The free CALB loses almost 90 % of its initial activity after 10 h, while the PMA-co-PAA@CTS-CALB still retains about 40 % of its activities. These results demonstrate that PMA-co-PAA@CTS-CALB has significant enhancement on the thermal stability compared with free CALB. This may be because the CTS-functionalized PMA-co-PAA could prevent enzyme from dissociating and aggregating.

#### Knoevenagel Condensation Reaction Catalyzed by PMA-co-PAA@CTS-CALB

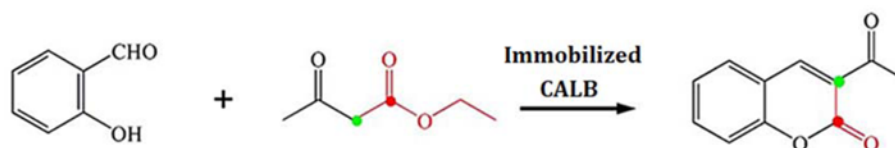
The Knoevenagel condensation reaction of salicylaldehyde and active methylene compound was chosen as a model reaction, PMA-co-PAA@CTS-CALB and CH<sub>3</sub>OH/H<sub>2</sub>O were used as catalyst and solvent, respectively (Scheme 2). Based on the current experiment, the reaction could provide

benzopyran derivative (Compound 3) in 73 % yield, while PMA-co-PAA@CTS fibers give no product and free CALB afford benzopyran derivative in 42 % yield.

The nature of the reaction medium has been regarded as an important parameter in lipase-catalyzed reaction. As shown in Table 1, the reaction in different organic solvents was examined. The catalytic activity of PMA-co-PAA@CTS-CALB in the Knoevenagel condensation reaction was remarkably influenced by the solvents. As shown in Table 1, the reaction in high-polarity solvents, such as water and CH<sub>3</sub>OH, give higher yields (Table 1, Entries 1 and 2) than in low-polarity solvents such as THF (Table 1, Entries 4). The yield of Knoevenagel condensation reaction in DMF or CH<sub>3</sub>CN is not examined due to the dissolution of the substrate PMA-co-PAA@CTS in these two solvents. As for DMF/H<sub>2</sub>O or CH<sub>3</sub>CN/H<sub>2</sub>O as solvent, the immobilized enzyme is quite stable. The yield is 10 % in DMF/H<sub>2</sub>O (Entry 7) and 15 % in CH<sub>3</sub>CN/H<sub>2</sub>O (Entry 8), which is higher than that of in water (5 %). This may result from the fact that the reactants of salicylaldehyde and thyl acetoacetate are favourable to dissolve in organic solvents than in water. However, water plays an important role in enzyme-catalysed organic reaction due to the fact that it provides a favourable environment for enzyme [30]. Thus, the impact of water

**Table 1.** The yield of the product at different reaction conditions

Entry	Solvent	Volume ratio	Time (h)	Yield (%)
1	H <sub>2</sub> O	-	4	5
2	CH <sub>3</sub> OH	-	4	5
3	DMF	-	4	-
4	CH <sub>3</sub> CN	-	4	-
5	THF	-	4	-
6	CH <sub>3</sub> OH/H <sub>2</sub> O	4:1	4	73
7	DMF/H <sub>2</sub> O	4:1	4	10
8	CH <sub>3</sub> CN/H <sub>2</sub> O	4:1	4	15
9	THF/H <sub>2</sub> O	4:1	4	5
10	CH <sub>3</sub> OH/H <sub>2</sub> O	1:1	4	40
11	CH <sub>3</sub> OH/H <sub>2</sub> O	2:1	4	48
12	CH <sub>3</sub> OH/H <sub>2</sub> O	6:1	4	56
13	CH <sub>3</sub> OH/H <sub>2</sub> O	8:1	4	58
14	CH <sub>3</sub> OH/H <sub>2</sub> O	4:1	1	46
15	CH <sub>3</sub> OH/H <sub>2</sub> O	4:1	2	65
16	CH <sub>3</sub> OH/H <sub>2</sub> O	4:1	6	70



**Scheme 2.** PMA-co-PAA@CTS-CALB catalyzed Knoevenagel condensation reaction for the formation of benzopyran derivative.



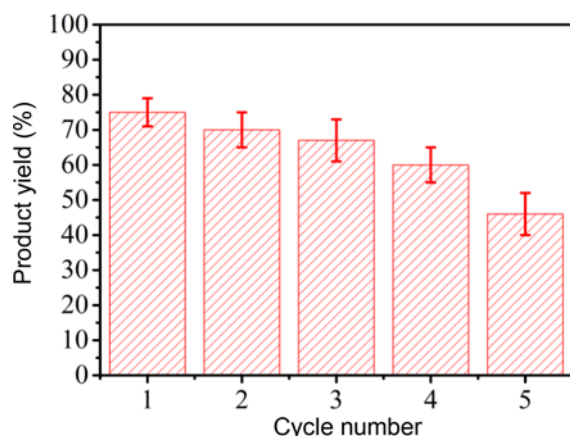


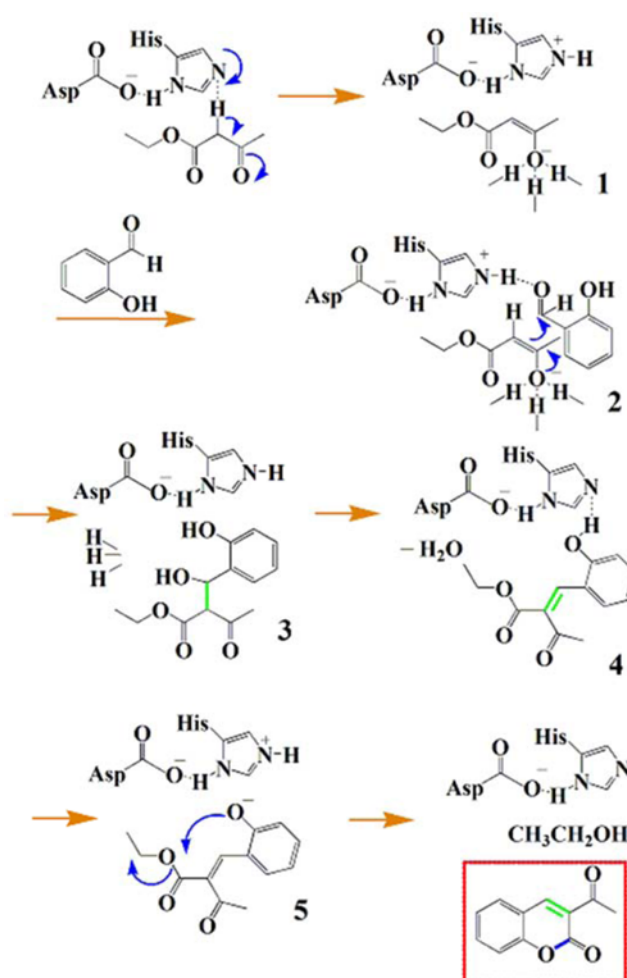
**Figure 4.** Reusability of the immobilized enzyme in Knoevenagel condensation reaction to produce benzopyran derivative.

content was investigated, and water contents from 0 to 100 % (v/v) were screened (Table 1, Entry 1-2, 6, 10-13). To this end, we were pleased to find that the reaction carried out at 20 % water (v/v) provided product 3 in 70 % yield (Table 1, Entry 6). The yield declined at higher or lower water contents (Table 1, Entry 10-14). As shown by the results, the active site of CALB is very sensitive to water, and water acts as a “molecular lubricant” for retaining the conformational flexibility of the immobilized CALB. Consequently, CH<sub>3</sub>OH/H<sub>2</sub>O (4/1 in v/v) was chosen as the solvent for further investigation. To further optimize the reaction conditions, the influence of reaction time were also investigated (Table 1, Entry 6, 14-16), which suggesting that the optimized reaction time is 4 h.

Reusability is the most important advantage of the immobilized CALB compared to other catalysts [31]. To evaluate their usability, the immobilized CALB was used in 5 cycles for the same reaction. As shown in Figure 4, the immobilized CALB shows good stability and retains more than 45 % of its initial activity over 5 consecutive reuses. In our case, the decrease in activity probably ascribed to the prolonged exposure of CALB to the organic solvent and the lipase loss during the reaction cycles [32].

### Possible Mechanism of Knoevenagel Condensation Reaction

A possible mechanism of Knoevenagel reaction was proposed based on our current experiments and previously reported works [33,34]. As presented in Scheme 3, firstly, enol form of Ethyl acetoacetate (Compound 1) was stabilized by the Asp-His dyad and oxyanion hole in the active site. Secondly, a proton was transferred from the enolate anion to the salicylaldehyde so as to form a new carbon-carbon bond. Thirdly, Compound 2 was generated through a Knoevenagel condensation. Then, it was further converted to Compound 3 via dehydration process with the assistance of the residue of



**Scheme 3.** The possible mechanism of cyclization reaction with the CALB catalyst.

CALB. Subsequently, the key precursor Compound 4 was released from Compound 3. Finally, the target product of benzopyran derivative was generated from the intramolecular nucleophilic addition within intermediate Compound 4.

### Conclusion

We demonstrate that CALB immobilized on chitosan-functionalized electrospun PMA-co-PAA membrane can be used as a “green” and recyclable biocatalyst for Knoevenagel condensation reaction. Chitosan tethered on the membrane surface can enhance the CALB loading amount without sacrificing the catalytic activity. As a result, the pH, thermal, and storage stabilities of the immobilized CALB are significantly improved. Moreover, a comparative study is conducted on the synthesis of benzopyran derivative by using immobilized and free CALB, revealing that the immobilized CALB exhibits a higher enzymatic catalyst activity than that of the free CALB. Notably, the Knoevenagel

condensation reaction in synthesis of benzopyran derivative can be significantly promoted by adding water in solvent, and the product yield can reach about 73 % under optimized water condition. Meanwhile, the immobilized CALB can function as a recyclable biocatalyst for synthesis of benzopyran derivative, which shows good stability over five cycles. As a green and efficient synthetic route, it not only expands the utility of lipase in organic synthesis but also serves as a potential synthetic approach for industrial application.

### Acknowledgements

This project was supported by grants from the National Natural Science Foundation of China (Nos. 21302001), Natural Science Research Project of Universities in Anhui Province (Nos. KJ2018A0124), the Key Program in the Youth Elite Support Plan in Universities of Anhui Province (Nos. gxyqZD2016119), and Youth Elite Support Plan of Anhui Polytechnic University (Nos. 2016BJRC013).

**Electronic Supplementary Material (ESM)** The online version of this article (doi: 10.1007/s12221-018-8200-5) contains supplementary material, which is available to authorized users.

### References

1. J. Kim, J. W. Grate, and P. Wang, *Trends Biotechnol.*, **26**, 639 (2008).
2. B. D. Ames, X. Liu, and C. T. Walsh, *Biochemistry*, **49**, 8564 (2010).
3. H. Wang, Z. Wang, C. Wang, F. Wang, H. Zhang, H. Yue, and L. Wang, *RSC Adv.*, **4**, 35686 (2015).
4. F. Yang, Z. Wang, H. Wang, H. Zhang, H. Yue, and L. Wang, *RSC Adv.*, **4**, 25633 (2015).
5. P. Adlercreutz, *Chem. Soc. Rev.*, **42**, 6406 (2013).
6. K. T. Ong, M. T. Mashek, S. Y. Bu, A. S. Greenberg, and D. G. Mashek, *Hepatology*, **53**, 116 (2011).
7. F. Yang, Z. Wang, X. Zhang, L. Jiang, Y. Li, and L. Wang, *ChemCatChem*, **7**, 3450 (2015).
8. H. Wang, Z. Wang, H. Zhang, G. Chen, H. Yue, and L. Wang, *Green Chem. Lett. Rev.*, **7**, 145 (2014).
9. A. C. Wu, P. Y. Wang, Y. S. Lin, M. F. Kao, J. R. Chen, J. F. Ciou, and S. W. Tsai, *J. Mol. Catal. B: Enzym.*, **62**, 235 (2010).
10. P. S. Van, R. Teeuwen, M. Janssen, R. Sheldon, P. Dunn, R. Howard, R. Kumar, I. Martinez, and J. Wong, *Green Chem.*, **13**, 1791 (2011).
11. I. Ardao, J. Comenge, M. D. Benaiges, G. Álvaro, and V. F. Puentes, *Langmuir*, **28**, 6461 (2012).
12. P. Steunenberg, M. Sijm, H. Zuilhof, J. P. Sanders, E. L. Scott, and M. C. Franssen, *J. Org. Chem.*, **78**, 3802 (2013).
13. K. Sugiyama, Y. Oki, S. Kawanishi, K. Kato, T. Ikawa, and M. Egi, *Cata. Sci. Tech.*, **6**, 5023 (2016).
14. C. Aouf, E. Durand, J. Lecomte, M. C. F. Espinoza, E. Dubreucq, H. Fulcrand, and P. Villeneuve, *Green Chem.*, **16**, 1740 (2014).
15. F. Yang, Z. Wang, H. Wang, C. Wang, and L. Wang, *RSC Adv.*, **5**, 57122 (2015).
16. F. Yang, H. Wang, L. Jiang, H. Yue, H. Zhang, Z. Wang, and L. Wang, *RSC Adv.*, **5**, 5213 (2015).
17. S. J. Mountford, A. L. Albiston, W. N. Charman, L. Ng, J. K. Holien, M. W. Parker, J. A. Nicolazzo, P. E. Thompson, and S. Y. Chai, *J. Med. Chem.*, **57**, 1368 (2014).
18. F. Yang, X. Zhang, F. Li, Z. Wang, and L. Wang, *Eur. J. Org. Chem.*, **2016**, 1251 (2016).
19. Y. Ding, X. Ni, M. Gu, S. Li, H. Huang, and Y. Hu, *Catal. Commun.*, **64**, 101 (2015).
20. Z. Wang, C. Y. Wang, H. R. Wang, H. Zhang, Y. L. Su, T. F. Ji, and L. Wang, *Chin. Chem. Lett.*, **25**, 802 (2014).
21. W. Chen, Z. Xie, H. Zheng, H. Lou, and L. Liu, *Org. Lett.*, **16**, 5988 (2014).
22. Y. Minami, M. Kanda, and T. Hiyama, *Chem. Lett.* **43**, 181 (2014).
23. F. A. Khan, J. Dash, R. Satapathy, and S. K. Upadhyay, *Tetrahedron Lett.*, **45**, 3055 (2004).
24. R. A. Sheldon and S. van Pelt, *Chem. Soc. Rev.*, **42**, 6223 (2013).
25. R. C. Rodrigues, C. Ortiz, A. Berenguer-Murcia, R. Torres, and R. Fernandez-Lafuente, *Chem. Soc. Rev.*, **42**, 6290 (2013).
26. D. Liang, B. S. Hsiao, and B. Chu, *Adv. Drug Del. Rev.*, **59**, 1392 (2007).
27. C. Li, L. Zhou, C. Wang, X. Liu, and K. Liao, *RSC Adv.*, **5**, 41994 (2015).
28. Y. Yang, J. Cui, M. Zheng, C. Hu, S. Tan, Y. Xiao, Q. Yang, and Y. Liu, *Chem. Commun.*, **48**, 380 (2012).
29. D. I. Rozkiewicz, Y. Kraan, M. W. T. Werten, F. A. Wolf, S. Vinod, B. J. Ravoo, and D. Reinhoudt, *Chem. Eur. J.*, **12**, 6290 (2006).
30. Z. B. Xie, N. Wang, and L. H. Zhou, *Chem. Cat. Chem.*, **5**, 1935 (2013).
31. X. Wu, C. Yang, J. Ge, and L. Zheng, *Nanoscale*, **7**, 18883 (2015).
32. E. Xun, X. Lv, W. Kang, J. Wang, H. Zhang, L. Wang, and Z. Wang, *Appl. Biochem. Biotech.*, **168**, 697 (2012).
33. S. Kłossowski, B. Wiraszka, S. Berłozęcki, and R. Ostaszewski, *Org. Lett.*, **15**, 566 (2013).
34. X. W. Feng, C. Li, N. Wang, K. Li, W. W. Zhang, Z. Wang, and X. Q. Yu, *Green Chem.*, **11**, 1933 (2009).